THE JOURNAL OF COMPARATIVE NEUROLOGY 383:473–488 (1997)

Glycine Immunoreactivity in the Lateral Nucleus of the Trapezoid Body of the Cat

GEORGE A. SPIROU[1,2]* **AND ALBERT S. BERREBI**[1,3]
[1]Department of Otolaryngology—HNS, West Virginia University School of Medicine, Morgantown, West Virginia 26506-9200
[2]Department of Physiology, West Virginia University School of Medicine, Morgantown, West Virginia 26506-9200
[3]Department of Anatomy, West Virginia University School of Medicine, Morgantown, West Virginia 26506-9200

ABSTRACT

The central auditory system contains several predominantly glycine-immunoreactive nuclei, and one of these, the lateral nucleus of the trapezoid body, contains cell bodies exhibiting a spectrum of labeling intensity. By using post-embedding glycine immunocytochemistry on thin sections, and toluidine blue staining of adjacent sections, we established that darkly glycine-immunoreactive neurons constituted a distinct morphological class and form one of three subnuclei of the lateral nucleus of the trapezoid body, called the posteroventral subnucleus. These neurons resemble, in both labeling intensity and cell body morphology, the principal cells of the medial nucleus of the trapezoid body. The other two subnuclei of the lateral nucleus of the trapezoid body, its main and hilus subnuclei, contained predominantly glycine-immunoreactive and glycine-immunonegative neurons, respectively. Glycine immunoreactivity was compared with γ-aminobutyric acid (GABA) immunoreactivity in order to identify other organizational features of the lateral nucleus of the trapezoid body. Cell bodies that displayed either dark glycine-immunoreactivity or which were glycine-immunonegative were GABA-immunonegative. Cell bodies that displayed GABA immunoreactivity were preferentially located in the main subnucleus. Patterns of distribution of axosomatic innervation in the lateral nucleus of the trapezoid body were revealed in which glycine-immunoreactive puncta were (1) more numerous than GABA-immunoreactive puncta on glycine-immunonegative cell bodies and (2) equal to or less numerous than GABA-immunoreactive puncta on glycine-immunoreactive cell bodies. The characteristics of neural circuitry revealed by glycine and GABA immunoreactivity in the lateral nucleus of the trapezoid body may be generalizable to other populations of neurons of the superior olivary complex and to other regions of the central nervous system containing glycinergic neurons, such as the retina. J. Comp. Neurol. 383:473–488, 1997.

Indexing terms: auditory pathways; brain stem; olivary nucleus; immunocytochemistry; neurotransmitters

Glycine and γ-aminobutyric acid (GABA) are considered to be the predominant neurotransmitters mediating fast synaptic inhibition in the central nervous system (for review, see Ottersen et al., 1995). Immunocytochemical probes reveal that glycine-like-immunoreactive (GLY-LI) neurons are most prevalent in the brainstem, spinal cord and retina (Campistron et al., 1986; Ottersen et al., 1986; Aoki et al., 1988). Within the brainstem, the auditory system is distinctive in containing numerous clusters of GLY-LI neurons in structures caudal to the inferior colliculus (Peyret et al., 1987; Wenthold et al., 1987; Aoki et al., 1988; Helfert et al., 1989; Saint Marie et al., 1989; Vater, 1995; Winer et al., 1995).

The most intensely GLY-LI cells of the auditory system and perhaps the entire central nervous system are the principal cells of the medial nucleus of the trapezoid body (MNTB) located medially within the superior olivary complex (Campistron et al., 1986; Wenthold et al., 1987; Aoki

Grant sponsor: National Institute on Deafness and Other Communication Disorders, N.I.H.; Grant numbers: DC01387, DC02266.

*Correspondence to: Dr. George A. Spirou, Department of Otolaryngology, West Virginia University School of Medicine, P.O. Box 9200, Morgantown, WV, 26506-9200. E-mail: gspirou@wvu.edu

Received 17 July 1996; Revised 24 March 1997; Accepted 26 March 1997

et al., 1988; Saint Marie et al., 1989; Luppi et al., 1991). Immunocytochemical studies have revealed that GLY-LI neurons are also distributed within the superior olive in the so-called periolivary nuclei, groups of cells that surround the principal cell groups of the superior olive, including the lateral nucleus of the trapezoid body (LNTB), the largest of the periolivary nuclei in cats (Peyret et al., 1987; Wenthold et al., 1987; Helfert et al., 1989; Ottersen et al, 1995). The LNTB contributes one of the major feedback projections to the cochlear nucleus (Spangler and Warr, 1991), and may also play a role in sound localization through recently described connections with the medial superior olive (Cant, 1991; Cant and Hyson, 1992). Recently, we identified three subnuclei of the LNTB based on cell morphology and afferent input patterns (Spirou and Berrebi, 1996). Knowledge of the neurochemical profiles of cells in each of the subnuclei is important to understanding their function, since the subnuclei may participate differentially in the diverse neural projections of the LNTB. Therefore, we investigated characteristics of glycine and GABA immunolabeling in the LNTB.

Immunocytochemistry yields varying labeling intensity among cells in a given preparation, the interpretation of which has been the subject of much discussion (Storm-Mathisen and Ottersen, 1990). In the retina, the intensity of GLY-LI correlates with morphological subclasses of amacrine cells (Pourcho and Goebel, 1990). Moreover, differences in the intensity of GLY-LI have been used to support the notion of morphological (and therefore functional) subclasses of small neurons in the dorsal cochlear nucleus (Osen et al., 1990; Moore et al., 1996). Previous studies of immunolabeling in the superior olive have noted the presence of darkly GLY-LI cells in the LNTB (Helfert et al., 1989; Saint Marie et al., 1989). A population of neurons called pale oval cells, which comprise the posteroventral subnucleus of the LNTB (pvLNTB), share Nissl staining characteristics and afferent innervation properties (contact via large synaptic terminals, at least some of which originate from cochlear nucleus bushy cells) with principal cells of the MNTB (Spirou and Berrebi, 1996). We explored the hypothesis that cells of the pvLNTB, like MNTB principal cells, exhibit dark GLY-LI, and may therefore share neurochemical attributes.

GABA-like-immunoreactivity (GABA-LI) in cell bodies is not as prevalent in the superior olive of cats and rodents as is GLY-LI (Helfert et al., 1989; Saint Marie et al., 1989). Since colocalization of GABA-LI and GLY-LI has been described for the cochlear nucleus (Osen et al., 1990; Kolston et al., 1992; Moore et al., 1996), we investigated the characteristics of GABA-LI in order to provide a complete profile of these inhibitory neurotransmitters within the LNTB. Arrangements of GLY-LI and GABA-LI puncta, presumed to represent primarily presynaptic boutons, may reveal functional features of neural circuitry. For example, one characteristic of the lateral superior olive is the tendency for GLY-LI cell bodies to be contacted by many fewer GLY-LI puncta than GLY-immunonegative cell bodies (Saint Marie et al., 1989), which may be a feature found in other auditory system structures (Winer et al., 1995) and GLY-LI amacrine cells of the retina (Hendrickson et al., 1988). Quantification of the arrangement of GLY- and GABA-immunoreactive puncta on LNTB cell bodies may underscore generalizable circuit patterns in structures receiving substantial glycinergic and GABAergic input.

MATERIALS AND METHODS

Five adult cats were used in these experiments. All animal protocols were approved by the Institutional Animal Care and Use Committee. Glycine and GABA immunocytochemistry was performed by using either a pre-embedding protocol (two animals) on frozen sectioned tissue or a post-embedding method (three animals) on plastic embedded tissue sections. In preparation for perfusion, animals were anesthetized by using a combination of Xylazine (10 mg) and Ketaset (10 mg/kg) and immobilized over a downdraft table.

Pre-embedding immunocytochemistry

Perfusion through the ascending aorta was performed by using 0.1 M sodium phosphate buffer (pH 7.1) followed by 2.5 liters of 1% paraformaldehyde and 2.5% glutaraldehyde in 0.1 M sodium phosphate buffer (pH 7.3, room temperature). The brain was dissected and placed in 30% sucrose in 0.075 M sodium phosphate buffer overnight.

Frozen sections were cut at 25 µm thickness in the coronal plane and collected, free-floating, in a series of wells. One series of sections was stained with cresyl violet; the remaining were processed for immunocytochemistry. Sections were rinsed in 0.5M Tris HCl (pH 7.6) and immersed for 1 hour in 5% normal donkey serum. Sections were then incubated with gentle agitation at 6°C in rabbit anti-glycine antiserum (dilution 1:1,000; purchased from Chemicon, Temecula, CA; antibody #139, lot numbers C4L093, 67295193, and 23896164) or a gift from Drs. J. Storm-Mathisen and O. Ottersen (University of Oslo; antibody #290) for 72 hours. After rinsing, the sections were incubated in a biotinylated secondary antibody and then processed by using the ABC method (Vector, Burlingame, CA). Following 5–15 minutes incubation in 3,3′ diaminobenzidine with hydrogen peroxide, sections were rinsed and dry mounted onto slides from gelatin alcohol.

Post-embedding immunocytochemistry

The vascular rinse was Ca^{2+}-free Ringer's solution followed by 3.5 liters of 2% paraformaldehyde and 2.5% glutaraldehyde in 0.1 M phosphate buffer at room temperature. Following perfusion, the head was removed and kept under ice for at least 1 hour prior to removal of the brain. The brain was dissected and left in fixative overnight.

The brainstem was cut into 150 µm sections in the coronal plane by using a Vibratome. These sections were postfixed with osmium tetroxide (0.5%), stained en bloc with aqueous uranyl acetate (2%), dehydrated and flat-embedded in Epon (Polybed 812, Polysciences). Thin (0.4 or 1.0 µm thick) plastic sections were cut through the superior olivary complex (SOC) and processed for immunocytochemistry or stained with toluidine blue. For immunocytochemistry, Epon was etched from the tissue by using 10-20% sodium hydroxide dissolved in ethanol (Lane and Europa, 1965). Osmium was removed from the sections with sodium periodate (1%). Sections were rehydrated and incubated overnight at 6°C with polyclonal rabbit antisera against bovine serum albumin-glutaraldehyde conjugates of glycine (Chemicon, Temecula, CA, 1:500–1:5,000) or GABA (gift of Dr. D. Pow, University of Queensland, Brisbane, Australia; 1:8,000); the remaining steps are as described above.

Specificity of antisera

Specificity of the above antisera (to glycine and GABA) used in the post-embedding protocol was determined by performing preadsorption controls by using amino acid-glutaraldehyde inhibitor complexes (Storm-Mathisen and Ottersen, 1990). Each antiserum was preadsorbed overnight with inhibitor complex solutions composed of 2–20 mM of either amino-acid conjugated to glutaraldehyde and then incubated with tissue sections as described above. GABA antiserum was tested by using sections of the cerebellar cortex (Fig. 1A–C) because GABA immunoreactive neural elements in this structure have been well characterized (Ottersen and Storm-Mathisen, 1984; Seguela et al., 1984; Somogyi et al., 1985). To test the glycine antiserum we employed sections containing principal cells of the MNTB (Fig. 1D–F), which are among the most intensely glycinergic neurons of the entire brainstem (Campistron, 1986; Wenthold et al., 1987; Helfert et al., 1989; Saint-Marie et al., 1989; Osen et al., 1990; Kolston et al., 1992). The glycine and GABA antisera did not show cross reactivity, and specific staining was eliminated by an excess of the targeted antigen. The specificity of these two antisera has been characterized by other authors in retina (Kallionatis and Fletcher, 1993; Pow and Robinson, 1994). All illustrations and data analysis utilized sections processed by using either the Chemicon glycine or GABA (D. Pow) antisera.

Identification of the subnuclei of the LNTB

Frozen (thick) sections. Cresyl violet stained sections adjacent to those reacted with glycine antisera were used to identify the three previously defined subnuclei of the LNTB: the main body of the LNTB (mLNTB), the posteroventral LNTB (pvLNTB), and the hilus region of the LNTB (hLNTB; Spirou and Berrebi, 1996). The border between the mLNTB and hLNTB runs along the ventral surface of the lateral superior olive parallel to the ventral brain surface.

Plastic-embedded (thin) sections. The pvLNTB contains a homogeneous population of cells that could be identified in toluidine blue labeled sections viewed under oil immersion (see Results). The ability to recognize the cells of the pvLNTB in thin sections was essential because their locations are not constant at all rostro-caudal levels. The border between the mLNTB and hLNTB was determined by using the same rule applied to the frozen sections.

Quantitative analysis

Optical density. Plastic-embedded sections were used for the following procedures. Densitometric analyses (Optimas, Inc., Edmonds, WA) were performed in selected sections on all cells of the LNTB and subsets of cells in other superior olivary nuclei to establish categories of GLY-LI intensity and to determine the percentage of cells that colocalize GLY-LI and GABA-LI. Two pairs of adjacent sections (at 0.4–1 μm thickness) from each of two animals were analyzed (four pairs total; 346 cells). One section of each pair was immunolabeled for glycine and the other for GABA. Images were captured directly from microscope slides by using a black and white camera (Dage CCD 72) and displayed on a video monitor. The average of the pixel grey values within each cell body was calculated and the density scale inverted so that a value of 0 indicated a white pixel and a value of 255 indicated a black pixel. Cells of the medial superior olive represented a good standard for immunonegativity, and cells of the MNTB represented a good standard for dark GLY-LI (Fig. 5).

We established three categories of GLY-immunolabeling: (1) dark GLY-LI, (2) light or medium GLY-LI, and (3) GLY-immunonegative. Inspection of the plots of optical density established a clear upper limit for immunonegativity (Fig. 5). The ability to predict, by using optical density data, that cells were located in either the MNTB or pvLNTB (dark GLY-LI) was determined by using logistic regression analysis and was highly significant (see Results). The statistical analysis verified the creation of the two categories of immunopositivity (dark; light or medium) based on densitometric analysis. In addition, three independent observers qualitatively judged the intensity of GLY-LI on two of these section pairs, by using the same three categories of immunolabeling. Nearly all of the cells (97%) were correctly categorized by all three evaluators, lending further credence to the clarity of the group boundaries and providing a basis for rapid, qualitative analysis of additional cells.

Next, qualitative assessment of glycine immunolabeling categories was performed on additional sections. For each cell, the GLY-LI was categorized and the cell was localized to one of the subnuclei of the LNTB by using an adjacent toluidine blue stained section (spacing between the GLY-LI and toluidine blue sections did not exceed 2 μm). Sections covering the rostro-caudal extent of the superior olivary complex were analyzed from two animals (animal #1: nine sections, 484 cells; animal #2: five sections, 264 cells). In a third animal, two sections were analyzed (73 cells), which confirmed the characteristic immunoreactivity patterns found in the first two animals. The percentage of cells in each subnucleus of the LNTB falling into each of the three categories of immunostaining intensity was determined from these sections. Comparisons among immunolabeling characteristics in the subnuclei were made by using a matched pairs *t*-test on the percentages.

Counts of immunolabeled puncta

We compared the numbers of GLY-LI and GABA-LI puncta contacting the somata of cells in each subnucleus of the LNTB and for each of the categories of immunolabeling. In addition, the number of GLY-LI and GABA-LI puncta contacting cell bodies of the MNTB and medial superior olive were counted to determine if characteristics of punctate immunolabeling in the LNTB were generalizable to other nuclei of the superior olive. Since the number of GLY-LI puncta apposed to GLY-LI and GLY-immunonegative cell bodies appeared to be so different, for a subset of cells in the LNTB, we also counted the number of puncta per 100 μm of cell perimeter in order to normalize for the varying size of cell profiles captured in a given tissue section. Counts of puncta and measurements of cell body perimeter were made from two sections in each of two animals, and cells were classified as being either GLY-LI (combination of the categories of dark and light or medium immunolabeling) or GLY immunonegative. All counts of puncta were made by using an oil immersion lens (100X objective) to identify the cell borders so that accurate counts, especially of immunolabeled endings onto immunolabeled cells, could be made. The ability to predict whether cells were GLY-LI or immunonegative from the number of glycine and GABA puncta on the cell body was performed

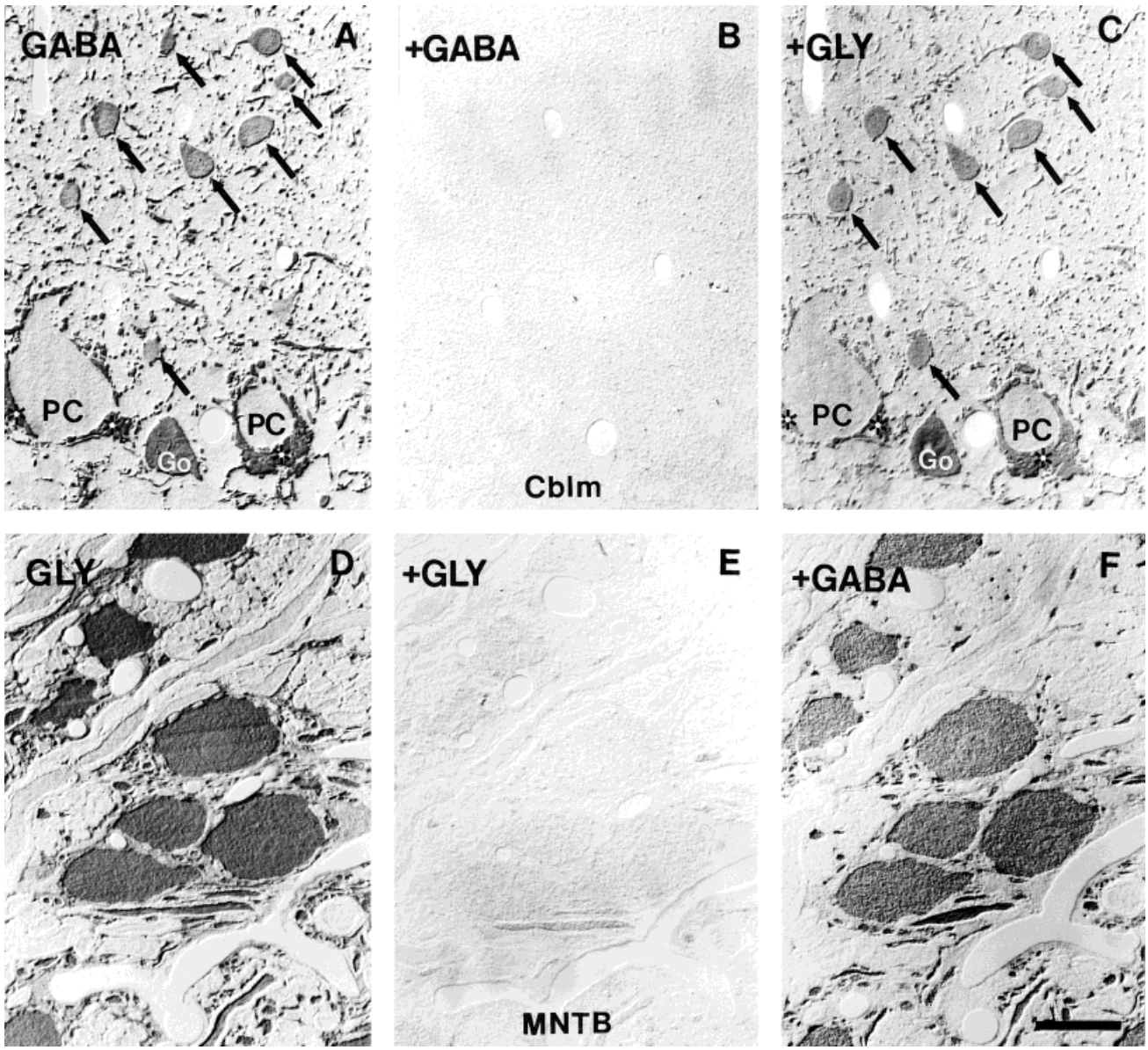

Fig. 1. Antibody specificity tests. The specificity of the γ-aminobutyric acid (GABA; A–C) and glycine (D–F) antibodies used in these studies was demonstrated by preadsorption tests by using amino acid-glutaraldehyde inhibitory complexes. Adjacent semithin sections (1.0 μm) of the cerebellum (Cblm) were used to test for specificity of the GABA antiserum and sections of the medial nucleus of the trapezoid body (MNTB) for the glycine antiserum. Sections that were free of reaction product could only be visualized effectively by using DIC optics. **A:** The GABA antiserum of Dr. D. Pow (University of Queensland) at a dilution of 1:8,000 gave specific immunoreaction product in the cerebellar cortex localized to stellate/basket cells (arrows) in the molecular layer and a subpopulation of Golgi interneurons (Go). Purkinje cells (PC) were lightly immunostained, but their outline was delineated clearly by a pericellular "basket" of axon terminals (small asterisks). Preadsorption of this antiserum overnight with 5 mM GABA inhibitor (**B**) completely abolished immunostaining, but preincubation with 5 mM glycine inhibitor (**C**) did not. **D:** The glycine antiserum purchased from Chemicon produced an intense immunoreaction product in cells of the medial nucleus of the trapezoid body (MNTB). Preincubation of this antiserum with 10 mM glycine inhibitor (**E**), but not with 10 mM GABA inhibitor (**F**), eliminated nearly completely this immunostaining. Scale bar = 30 μm.

by using logistic regression analysis (see Results). In addition, the number of GLY-LI puncta per length of the cell perimeter in GLY-immunolabeled thin sections was quantified by counting puncta apposed to a cell and measuring the length of the cell perimeter by using a drawing tablet (Optimas). Statistical analysis was performed by using JMP software, a registered trademark of the SAS Institute (Cary, NC).

RESULTS

Overview of GLY-immunolabeling

Pre-embedding protocol. GLY-LI in the superior olivary complex of the cat was observed in cell bodies, fibers and puncta which vary in labeling intensity (Fig. 2). GLY-LI neurons were prevalent in the MNTB and they also constituted a subpopulation of cells in the lateral

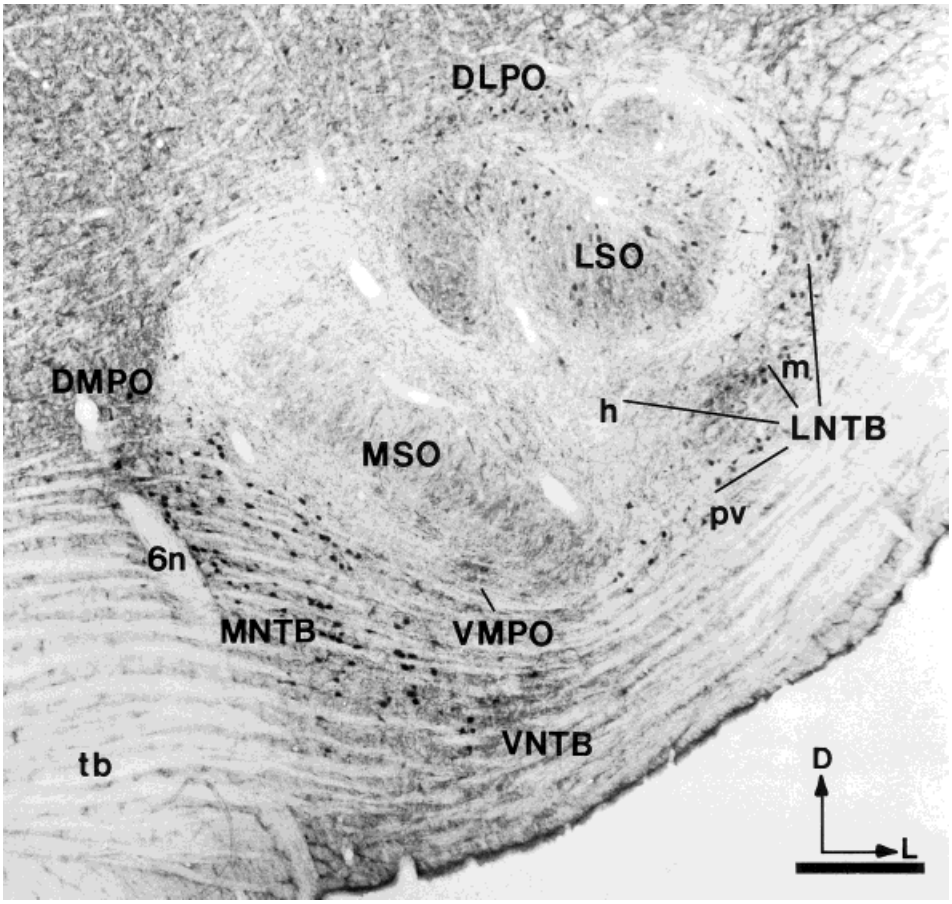

Fig. 2. Overview of glycine-like-immunoreactivity (GLY-LI) in the cat superior olivary complex. Frozen section, immunoreacted by using a pre-embedding protocol. The MNTB is easily recognized due to the intense GLY-LI of its principal neurons. The LSO is identified by an immunolabeled neuropil and scattered GLY-LI cells within the nucleus. Neurons of the MSO are GLY-immunonegative. Several of the periolivary nuclei, such as the LNTB (three subnuclei: m indicates the mLNTB, pv indicates the pvLNTB, h indicates the hLNTB), DLPO, and VNTB, contain large numbers of GLY-LI cell bodies. Other periolivary nuclei, such as the DMPO and VMPO, contain mostly immunonegative cells. Abbreviations: LNTB, lateral nucleus of the trapezoid body; MNTB, medial nucleus of the trapezoid body; LSO, lateral superior olive; MSO, medial superior olive; VNTB, ventral nucleus of the trapezoid body; DLPO, dorsolateral periolivary nucleus; DMPO, dorsomedial periolivary nucleus; VMPO, ventromedial periolivary nucleus; D, dorsal; L, lateral; 6n, sixth cranial nerve root; tb, trapezoid body. Scale bar = 0.5 mm.

superior olive. Cells of the medial superior olive and ventromedial periolivary nucleus were immunonegative, in accord with previous reports (Wenthold et al., 1987; Helfert et al., 1989; Saint Marie et al., 1989). However, GLY-LI neurons were found in other periolivary nuclei, including the LNTB, ventral nucleus of the trapezoid body, and the dorsolateral and dorsomedial periolivary nuclei. Additional periolivary nuclei in the lateral part of the superior olivary complex, namely the posterior periolivary nucleus (Fig. 4) and anterolateral periolivary nucleus (not shown) contained both GLY-LI and GLY-immunonegative cells. Within the LNTB, two subnuclei, the main body of the LNTB (mLNTB) and posteroventral LNTB (pvLNTB) contained the majority of GLY-LI cells, and the third subnucleus, the hilus region of the LNTB (hLNTB), contained very few immunoreactive cells (Fig. 2). Neuropil immunolabeling was found in all nuclei of the superior olive, appearing especially dense in the dorsomedial and ventromedial periolivary nuclei, ventral nucleus of the trapezoid body and portions of the lateral superior olive, medial superior olive, and LNTB, although fibers of the trapezoid body were largely immunonegative. The remainder of this report is focused on the glycine immunolabeling characteristics of the LNTB in comparison to patterns found in the principal nuclei of the superior olive.

Post-embedding protocol. In thin sections, the cell cytoplasm is exposed at the cut surface of the slice and immunoreagents have optimal access to intracellular antigens throughout the tissue, permitting accurate descriptions of the relative intensity of immunolabeling among cellular structures. The limited thickness ($\leq$ 1.0 μm) of the tissue section reveals clearly the cytological features needed to make correlations between morphology and intensity of immunoreactivity. In addition, individual punctate profiles, presumably representing presynaptic boutons as well as cross-cut axons, can be visualized on consecutive sections processed using different antisera or stained with toluidine blue. For these reasons, the remaining descriptions of GLY-and GABA-LI will be made using material processed using the post-embedding protocol. In accord with immunolabeling patterns observed in frozen sections, the postembedding protocol revealed darkly immunoreac-

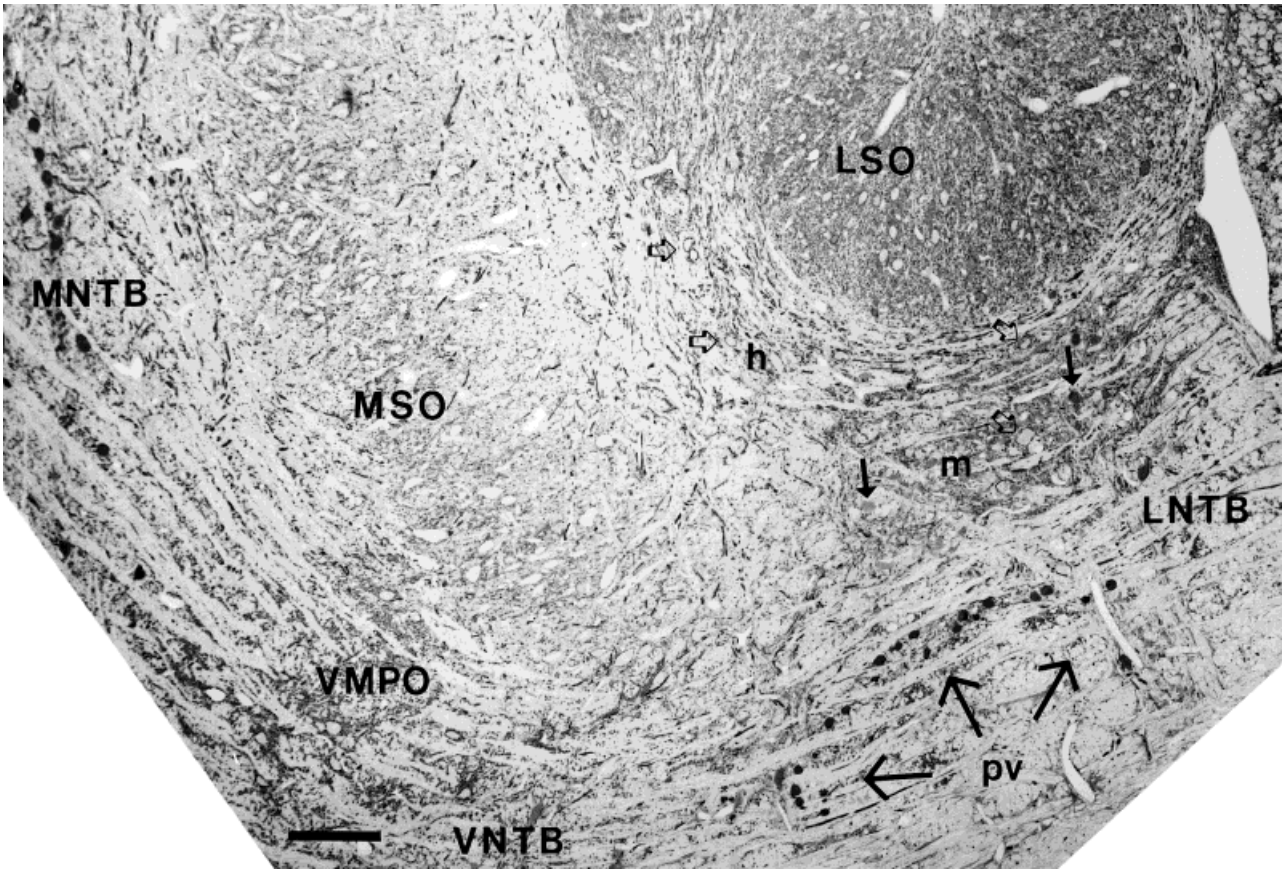

Fig. 3. Distribution of GLY-LI in the superior olivary complex; post-embedding protocol. The greatest variation in the intensity of GLY-LI is found within cell bodies in the LNTB. A population of cells comprising the pvLNTB (large arrows at lower right) are as darkly immunolabeled as principal cells of the MNTB. Light to medium intensity of immunolabeling is observed in the mLNTB (small arrows), LSO and VNTB, and immunonegative cells are distributed in the mLNTB, hLNTB (open arrows), MSO, and VMPO. Orientation same as in Figure 1. Abbreviations as in Figure 2. Scale bar = 0.2 mm.

tive principal cells of the MNTB (Figs. 3, 4) located medial to the immunonegative cells of the medial superior olive, the latter of which were made conspicuous by the presence of GLY-LI puncta outlining their perimeter. Both light to medium GLY-LI and GLY-immunonegative cells were present in the lateral superior olive, together with a dense collection of GLY-LI fibers and puncta.

Lateral nucleus of the trapezoid body

pvLNTB. The salient feature of GLY-LI in the LNTB was the presence of a homogeneous group of small oval cells whose intensity of immunolabeling rivals that of principal cells of the MNTB (Figs. 3, 4, 5B,D,E). These cells were concentrated caudally and ventrally and their spatial distribution closely matched the extent of the pvLNTB subnucleus. The basis for concluding that the darkly GLY-LI cells were pvLNTB cells is documented in a later section.

mLNTB. The many GLY-LI cells that were found within the largest subdivision of the LNTB, the mLNTB, had a variety of shapes, sizes and intensity of immunolabeling (Figs. 3, 4, 6B,D). However, few cells matched the intensity of immunolabeling found in the pvLNTB. Immunonegative cells were scattered throughout the mLNTB, but these tended to be located dorsally, near the lateral superior olive (Fig. 3).

hLNTB. The smallest subnucleus of the LNTB, the hLNTB, is also composed of cells having a variety of shapes and sizes, the great majority of which were immunonegative (Figs. 3, 6F). The somata of hLNTB cells, and GLY-immunonegative cells of the mLNTB, were outlined clearly by GLY-LI puncta. Fiber and punctate immunolabeling appeared less dense in the hLNTB than in the adjacent mLNTB (Fig. 3); many of the GLY-LI fibers seen in the hLNTB entered the lateral superior olive through its ventral hilus.

Delineation of LNTB subnuclei in toluidine blue stained thin sections

In order to correlate glycine immunoreactivity patterns with morphological features of cells, we determined criteria for recognizing pvLNTB cells in toluidine blue stained thin sections. In thin sections, these cells were characterized by an oval shape, smooth nuclear membrane, and a clearly defined nucleolus. The distribution of intracellular organelles gave their cytoplasm a rather homogeneous appearance (Fig. 5C). Cells of the pvLNTB often formed small clusters of two to three neurons in the caudal and ventral LNTB, and large puncta ($> 6\ \mu m^2$) were often found in apposition to their somata (Fig. 5C). MNTB principal cells had a similar appearance in toluidine blue

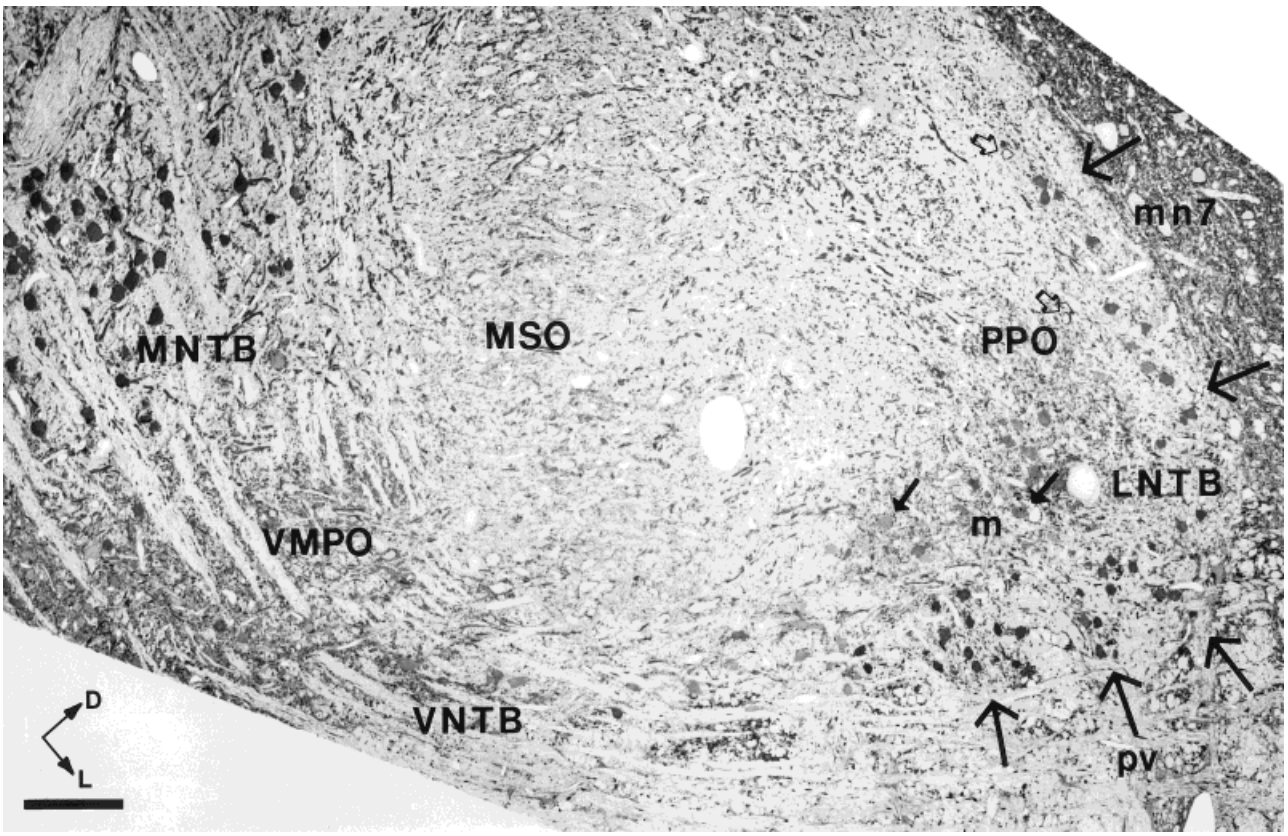

Fig. 4. GLY-LI in the caudal portion of the superior olivary complex; post-embedding protocol. Darkly immunoreactive cells of the pvLNTB are concentrated at this level and form dorsal (two large arrows at upper right) and ventral populations (indicated by three large arrows at lower right), separated by more lightly immunoreactive (small arrows) and immunonegative cells (open arrows) of the mLNTB and PPO. Darkly immunoreactive cells of the MNTB are seen at left. The immunonegative cells of the MSO and VMPO are evident, as are immunopositive cells of the VNTB. Abbreviations as in Figure 2 except: PPO, posterior periolivary nucleus; mn7, motor nucleus of the seventh cranial nerve. Abbreviations as in Figure 2. Scale bar = 0.2 mm.

stained sections, although they were larger than pvLNTB cells. MNTB principal cells were also apposed to large punctate profiles, which reflected the appearance in cross-section of synaptic endings that comprise the calyces of Held (Fig. 5A). Cells from the mLNTB (Fig. 6A, C) and hLNTB (Fig. 6E) were variously sized and displayed large, conspicuous clumps of pale staining material within their cytoplasm, which presumably represented stacks of granular endoplasmic reticulum (Peters et al., 1991). Furthermore, their nuclear membranes could be either smooth or indented. We were not able to distinguish further between cells of the mLNTB and hLNTB or to describe subpopulations of cells within these subnuclei.

Overview of GABA immunolabeling

Overall, GABA-LI in cell bodies of the superior olivary complex was much less prevalent than GLY-LI. The patterns of fiber and punctate labeling appeared less organized, in that they did not reveal boundaries of cell groups, in contrast to the clear outlines identifiable with GLY-LI. Within the LNTB, cell bodies with light to medium immunolabeling intensity were found, but no cells rivaled the dark GLY-LI found in the MNTB and pvLNTB.

Quantification and colocalization of GLY-LI and GABA-LI in cell bodies

The intensity of GLY-LI and GABA-LI in adjacent sections containing the MNTB, medial superior olive and the LNTB was quantified by measuring optical density (Fig. 7). Cells of the medial superior olive, hLNTB (Fig. 6F) and subsets of cells from the mLNTB and lateral superior olive had the lowest optical density of both GLY-LI and GABA-LI, and served to define the threshold for immunopositivity. Most cells of the mLNTB (Fig. 6B,D) displayed GLY-LI and had intermediate optical densities. Cells of the MNTB (Fig. 5B), pvLNTB (Fig. 5D,E) and a few cells of the mLNTB had the highest optical density of GLY-LI. In order to verify the relationship of immunostaining intensity with cell morphology, the data were divided into two groups: (1) pvLNTB and MNTB cells and (2) all other cells. Logistic regression analysis was used with group membership as the response and glycine and GABA intensity as predictors. For all four cases (pairs of sections), glycine, but not GABA, intensity was significantly associated with group membership ($P < .001$ level, likelihood ratio chi square). The error rates for the four cases were 4/98 cells, 9/89 cells, 2/88 cells, and 5/71 cells. Thus, intense GLY-LI within the superior olivary complex was associated with pvLNTB and MNTB cells.

A summary of the prevalence of GLY-LI and its intensity among the subnuclei of the LNTB for three animals is presented in Table 1. Nearly all cells (range 98–100%) of the pvLNTB were GLY-LI and nearly all of these (range 91–100%) were classified as having dark immunolabeling. Most cells of the mLNTB (range 77–92%) were GLY-LI, and of these nearly all were classified as having light or

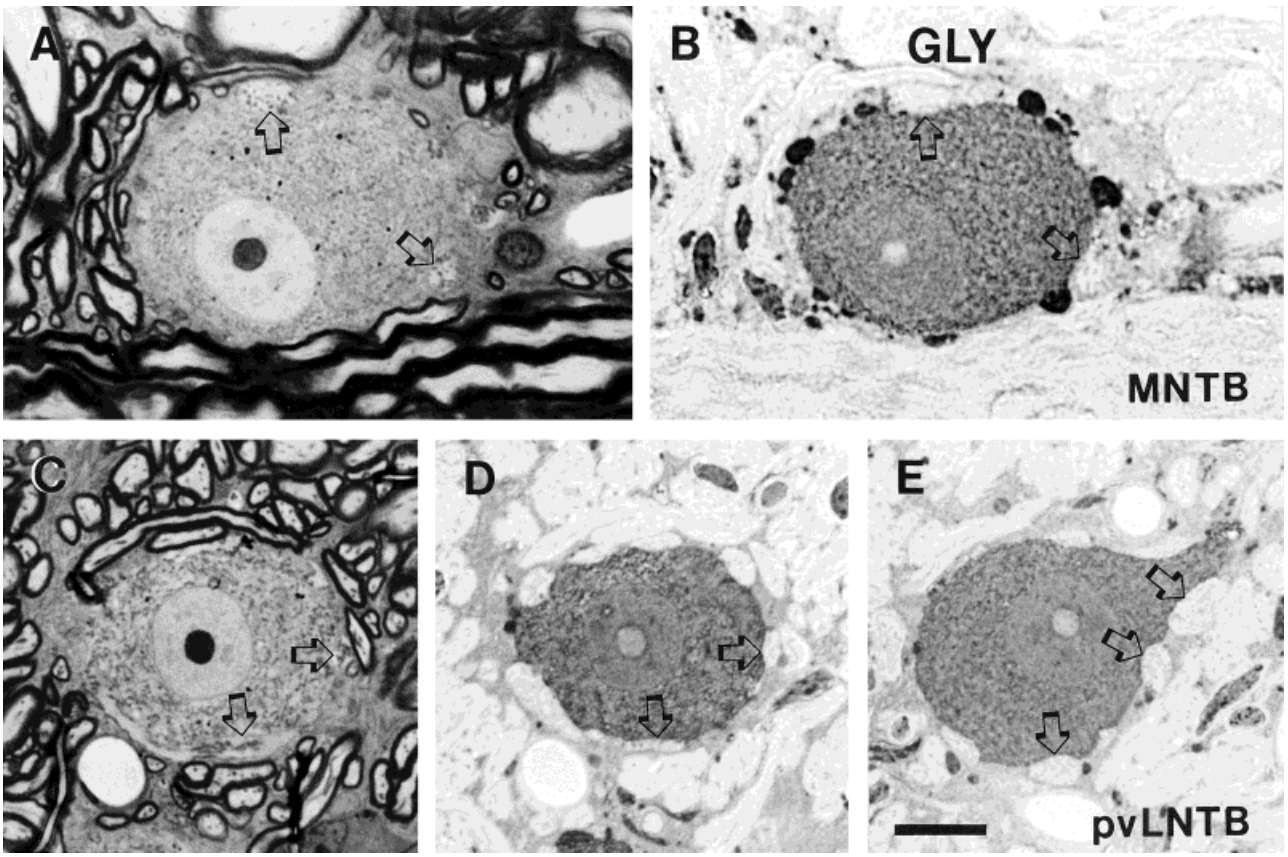

Fig. 5. Cells of the MNTB (A,B) and pvLNTB (C–E) have a similar appearance in toluidine blue stained (A,C) sections and display dark GLY-LI (B,D,E). MNTB and pvLNTB neurons have smooth nuclear membranes and a prominent nucleolus. The uniform distribution of their intracellular organelles lends a homogeneous appearance to their cytoplasm in toluidine blue stained sections. Large puncta (open arrows) represent calyceal terminals on cells of the MNTB (A) and are GLY-immunonegative (open arrow in B). **A,B:** Adjacent sections through the same cell. GLY-LI puncta can be seen apposed to the cell bodies. **C**: Large puncta are also apposed to cell bodies of pvLNTB neurons (open arrows); an axon appearing to give rise to a synaptic terminal is captured along the underside of this cell. **D:** These large puncta are GLY-immunonegative (open arrows). C,D: Sections through the same cell, separated by 0.4 µm. **E**: Another cell of the pvLNTB, showing dark GLY-LI and large immunonegative puncta (open arrows) apposed to the cell body and proximal dendrite. Abbreviations as in Figure 2. Scale bar = 10 µm.

medium immunolabeling. Very few cells (range 0–8%) of the hLNTB were GLY-LI and all of these had light or medium immunolabeling. Therefore, with few exceptions, the greatest percentage of and the darkest GLY-LI cells were found in the pvLNTB.

Another means of documenting this result is to plot the spatial distribution and GLY-LI characteristics of all neurons in the LNTB in representative sections (Fig. 8). The close correspondence of immunolabeling intensity with the boundaries of the subnuclei of the LNTB is most easily appreciated in sections through the mid-superior olive (containing the lateral superior olive; lower two panels of Fig. 8), since all three subnuclei are found at these levels.

Colocalization of GLY-LI with GABA-LI. As mentioned previously, very few neurons of the superior olive showed dark GABA-LI (Fig. 7). Cells within the LNTB that were immunolabeled using GABA antiserum were found predominantly in the mLNTB and were GLY-LI (Figs. 7, 9). Using optical density measurements, approximately 44 ± 13% (mean ± s.d., n = 4 section pairs) of the GLY-LI mLNTB cells displayed GABA-LI. Cells that were GLY-immunonegative were also GABA-immunonegative;

TABLE 1. Characteristics of Glycine Immunolabeling in the LNTB[1]

LNTB subnucleus	Proportion GLY-LI	Proportion classified as darkly GLY-LI
pvLNTB		
Animal #1	(177/180) 98%	(167/177) 94%
Animal #2	(77/78) 99%	(70/77) 91%
Animal #3	(34/34) 100%	(34/34) 100%
mLNTB		
Animal #1	(230/300) 77%	(17/230) 7%
Animal #2	(159/173) 92%	(6/159) 4%
Animal #3	(34/39) 87%	(0/34) 0%
hLNTB		
Animal #1	(4/51[2]) 8%	(0/4) 0%
Animal #2	(0/13) 0%	(0/0) 0%
Animal #3	—	—

[1]Percentage of glycine-like-immunoreactive (GLY-LI) neurons in the subnuclei of the lateral nucleus of the trapezoid body (LNTB) and the percentage of neurons with dark GLY-LI characteristics. Evaluations were made qualitatively, from three animals, as described in the Methods. Differences among groups was ascertained by using a matched pairs t-test on percentages from each animal. Column 2: The proportion of GLY-LI cells in the posteroventral subnucleus of the LNTB (pvLNTB) differed from the proportion in the main subnucleus of the LNTB (mLNTB; $P < .05$) and the hilus subnucleus of the LNTB (hLNTB; $P < .001$). Column 3: The proportion of darkly GLY-LI cells in the pvLNTB differed from the proportions in the mLNTB or hLNTB ($P < .001$).

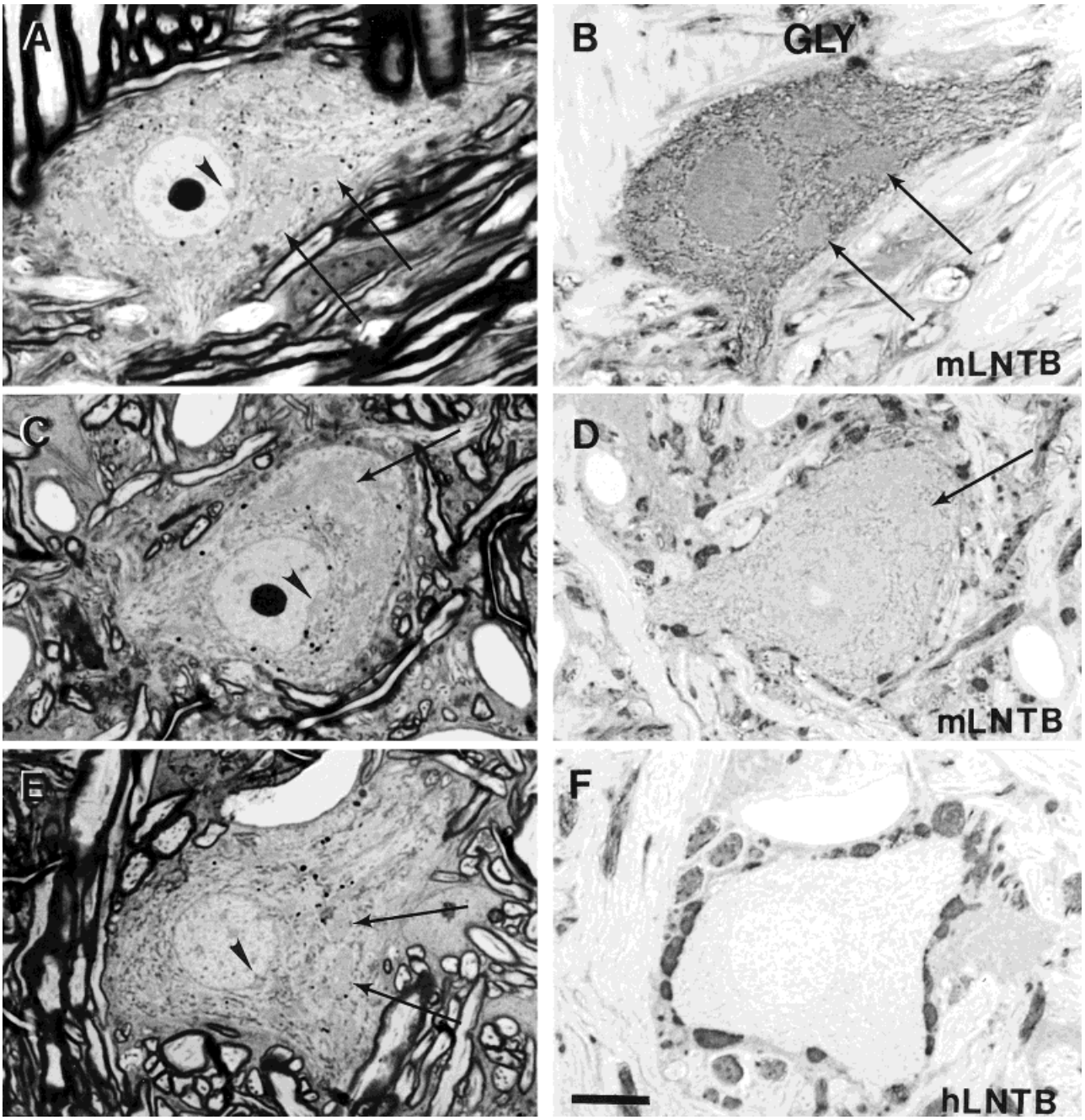

Fig. 6. Cell bodies of the mLNTB and hLNTB display a range of morphologies as revealed by toluidine blue staining and differing intensities of GLY-LI. (**A**,**C**) mLNTB and (**E**) hLNTB cells can have smooth or indented (arrowheads) nuclear membranes. The cytoplasm of these cells contains large, conspicuous clumps of pale staining organelles, presumably representing stacks of endoplasmic reticulum (thin arrows; also evident in **B**,**D**). Right hand panels are sections through the same cells, separated by 0.4 µm. Most cells of the mLNTB exhibit medium (B) or light (D) GLY-LI. Most cells of the hLNTB (**F**) are immunonegative and are outlined by numerous GLY-LI puncta, some of which appear quite large. Abbreviations as in Figure 2. Scale bar = 10 µm.

therefore, cells of the hLNTB were largely immunonegative for both antisera. The great majority of cells of the pvLNTB were GABA-immunonegative, as were cells of the MNTB and medial superior olive.

Punctate Immunolabeling

GLY-LI puncta were found throughout the LNTB in association with cell bodies in each of the categories of glycine immunostaining (Figs. 5, 6). GLY-immunonegative cells appeared to be contacted by more GLY-LI puncta than immunopositive cells (Fig. 6B,D,F), a feature that was borne out by counting puncta on a subset of LNTB cells whose perimeter length was quantified (Table 2). The numbers of GLY-LI puncta per 100 µm length of cell membrane on immunonegative cells located in the hLNTB and mLNTB (animal #1: 15.10 ± 8.4/100 µm, n = 27 cells;

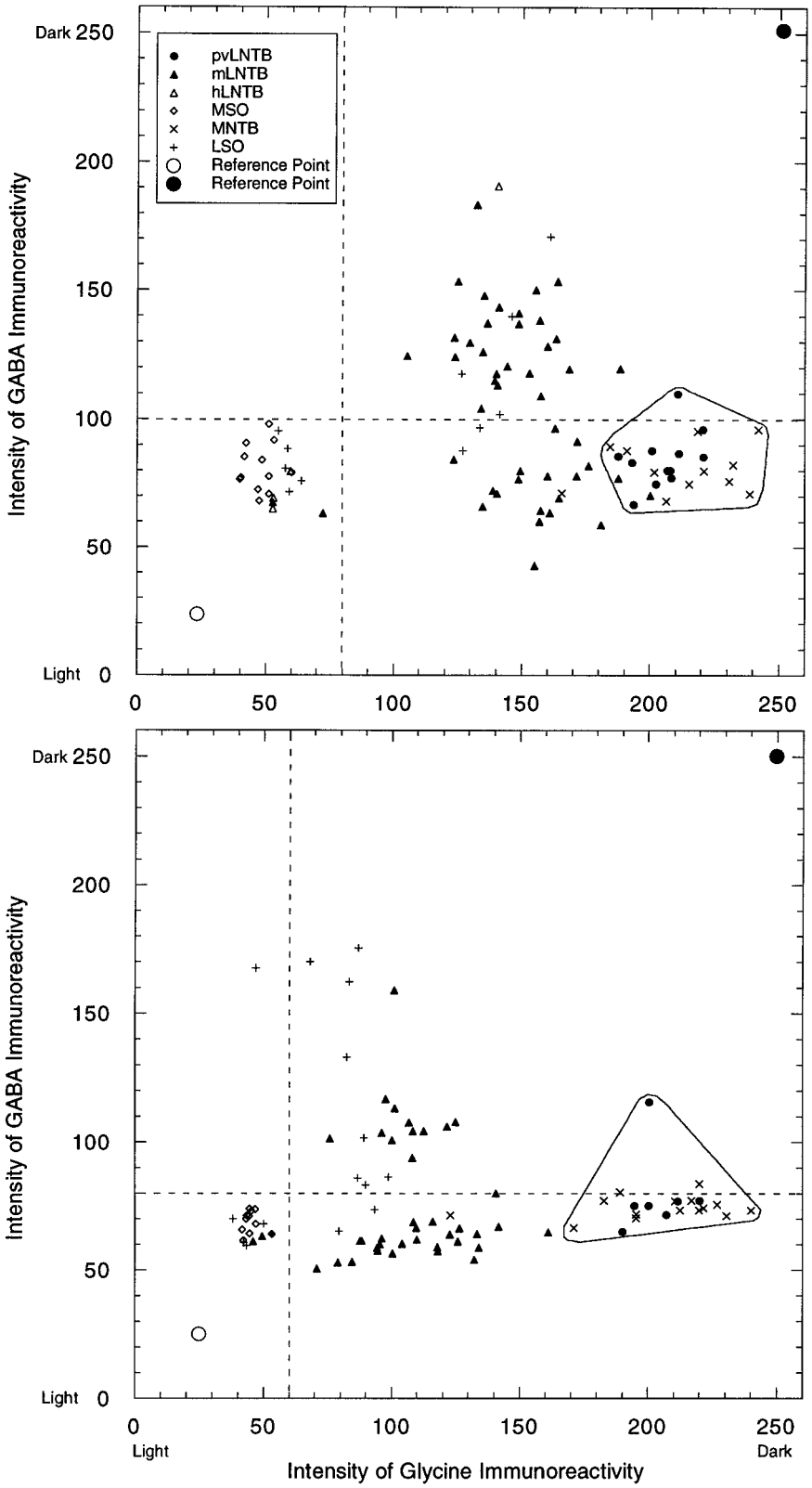

Fig. 7. Optical density of GLY-LI and GABA-LI for cells of the LNTB (each of three subdivisions), MSO, MNTB, and LSO. Each plot is from a separate cat; each pair of sections was taken from a coronal series through the middle one-third of the rostro-caudal extent of the superior olive. Cells of the medial superior olive, the hLNTB and some cells of the mLNTB and lateral superior olive form a cluster at the lower left of the plot and define the range of pixel grey values considered immunonegative, which are marked as the horizontal and vertical dashed lines on the graph. Cells of the MNTB and pvLNTB exhibit dark GLY-LI, are GABA immunonegative and are encircled (except for one outlying cell in top plot) at the right part of each plot. Most cells of the mLNTB have intermediate GLY-LI grey values, although a few cells have dark GLY-LI, and some cells are immunonegative. Roughly one-third to half of the mLNTB cells exhibit GABA-LI (58% in top plot; 32% in bottom plot). Reference points were dark immunolabeled fibers in each section (solid circle at upper right) and the space within a large blood vessel (open circle at lower left). Measurements were taken from pairs of adjacent, 0.4 µm sections. Measurements taken from an additional pair of adjacent sections in each cat have a similar distribution (not shown). Abbreviations as in Figures 1 and 2.

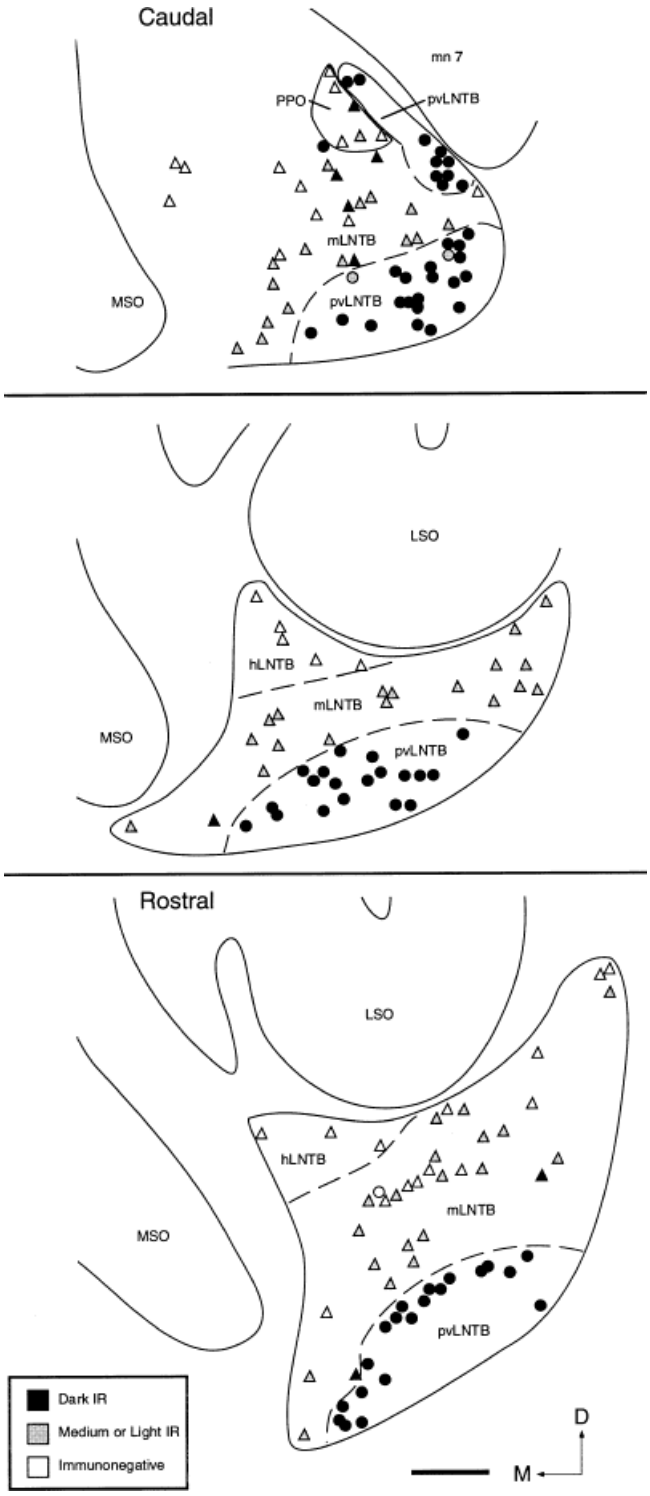

Fig. 8. Cells displaying different intensities of GLY-LI are segregated among the three morphologically defined subnuclei of the LNTB. Intensity of GLY-LI is indicated by amount of shading. Pale oval cells of the pvLNTB (mostly dark GLY-LI) are indicated by circles; those of the mLNTB (medium or light GLY-LI or GLY immunonegative) and hLNTB (GLY-immunonegative) by triangles. Sections taken caudal to the lateral superior olive (**top**), through caudal one-third of the lateral superior olive (**middle**), and through the rostral one-third of the lateral superior olive (**bottom**). Pale oval cells of the pvLNTB are not found rostral to the lateral superior olive. Abbreviations as in Figures 2 and 3. Scale bar = 0.2 mm.

animal #2: 24.0 ± 9.5/100 μm, n = 12 cells; mean ± s.d.) was more than twice that found on GLY-LI cells in the mLNTB (animal #1: 5.66 ± 4.2/100 μm, n = 64 cells; animal #2: 4.34 ± 3.0/100 μm, n = 60 cells) and pvLNTB (animal #1: 6.23 ± 4.0/100 μm, n = 81 cells; animal #2: 6.48 ± 2.8/100 μm, n = 20 cells). GLY-LI puncta in some cases were quite large (Fig. 6F), approaching the size of the large GLY and GABA-immunonegative puncta contacting MNTB and pvLNTB cells (Fig. 5B,D,E).

The relative numbers of GLY-LI and GABA-LI puncta contacting cell bodies in the LNTB, MNTB and medial superior olive varied depending on whether the cell body showed GLY-LI or GLY-immunonegativity (Fig. 9). Within the LNTB, GLY-LI cells (pvLNTB, mLNTB) were apposed to GABA-LI puncta that equalled or exceeded the number of GLY-LI puncta. However, GLY-immunonegative cells (mLNTB, hLNTB) were apposed to more GLY-LI than GABA-LI puncta (Fig. 10A,C). The same trends were evident when comparing GLY-LI cells of the MNTB to GLY-immunonegative cells of the MSO (Fig. 10B,D). Comparisons between groups (GLY-LI or GLY-immunonegative) were made with the number of GLY-LI puncta and the number of GABA-LI puncta as predictors. The number of GLY-LI puncta alone predicted group membership ($P < .05$, likelihood ratio chi square), although in one comparison (Fig. 10D) the number of both GLY-LI and GABA-LI puncta was required to reach significance ($P < .01$). Therefore, glycine immunolabeling of the cell body was highly correlated with the extent of somatic contact by GLY-LI and GABA-LI puncta.

DISCUSSION

Specificity of immunolabeling

One issue that must be addressed in any immunocytochemical study is the specificity of immunostaining. We performed our tests of the antisera using tissue well characterized for GABA-LI (cerebellar cortex; Ottersen and Storm-Mathisen, 1984; Seguela et al., 1984; Somogyi et al., 1985) and GLY-LI (MNTB; Campistron et al., 1986; Wenthold et al., 1987; Helfert et al., 1989; Saint Marie et al., 1989). Preadsorption of each antiserum with glycine or GABA-glutaraldehyde conjugates demonstrated both specific staining and a lack of cross reactivity. Thus, we have confidence in concluding that the antisera used in this study specifically revealed glycine and GABA.

Interpretation of GLY immunolabeling intensity

Interestingly, the patterns of GLY-LI differ significantly among the three subnuclei of the LNTB, whose boundaries were established independently (Spirou and Berrebi, 1996) and, therefore, provides supportive evidence for this parcellation of the LNTB. Dark GLY-LI is associated with the pvLNTB; light to medium GLY-LI is associated with the mLNTB; GLY-immunonegativity is associated with the hLNTB. Since distinct populations of cells are immunonegative, in general the metabolic pools of glycine appear to be below the detection limit of standard light microscopic immunocytochemical procedures. Therefore, variations in immunostaining intensity raise questions about whether one set of neurons can be more "glycinergic" than another. Variations in immunolabeling intensity could be due to a variety of factors, which may include (1) the presence of large cellular pools of amino acids other than

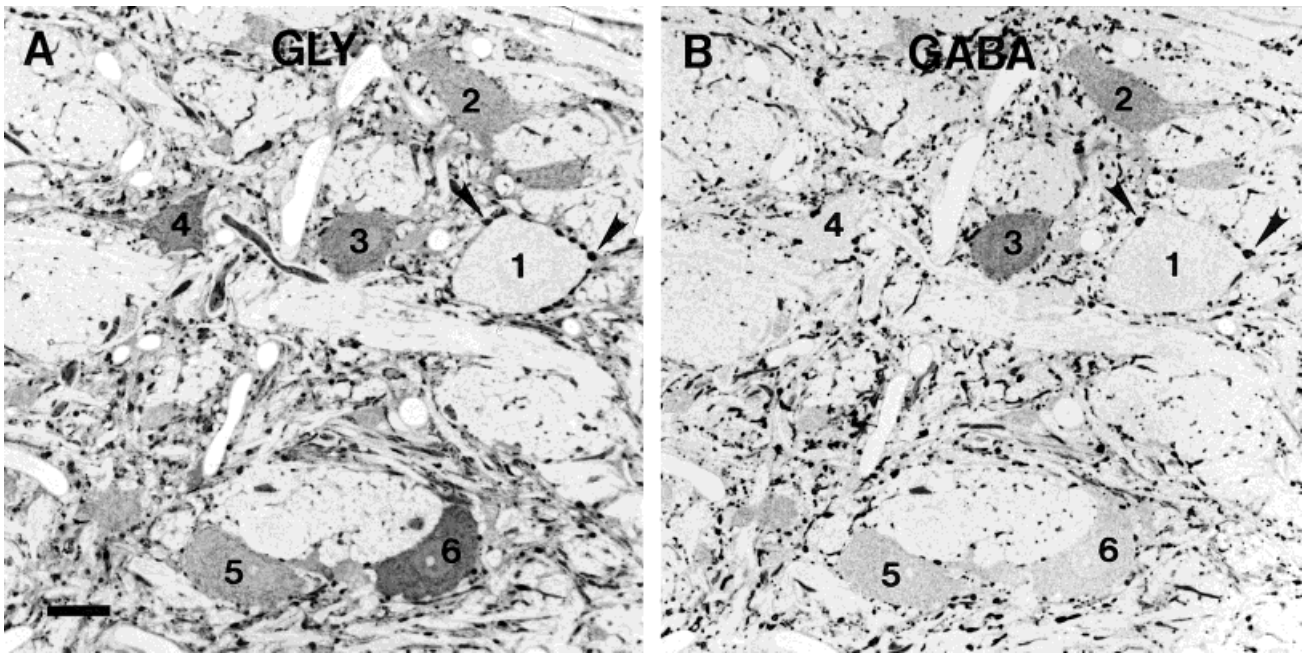

Fig. 9. Comparison of (**A**) GLY-LI and (**B**) GABA-LI in the mLNTB on adjacent 0.4 µm sections. GLY-immunonegative cells are GABA-immunonegative (cell 1). Cells having GLY-LI can exhibit a medium intensity of GABA-LI (cells 2, 3), be GABA-immunonegative (cell 4) or show light GABA-LI (cells 5, 6). The colocalization of GLY-LI and GABA-LI in puncta is most apparent on the few GLY-immunonegative cells in this subnucleus (arrowheads in A and B). Abbreviations as in Figures 1 and 2. Scale bar = 20 µm.

TABLE 2. GLY-LI Puncta Apposed to Cell Bodies of the LNTB[1]

Number of puncta per 100 µm cell perimeter			
	Immunonegative cell bodies	Immunopositive cell bodies	
	m-hLNTB	mLNTB	pvLNTB
Animal #1	15.10 ± 8.4 n = 27	5.66 ± 4.2 n = 64	6.23 ± 4.0 n = 81
Animal #2	24.0 ± 9.5 n = 12	4.34 ± 3.0 n = 60	6.48 ± 2.8 n = 20

[1]GLY-LI puncta apposed to GLY-LI and GLY-immunonegative cell bodies were counted and the cell perimeter measured as described in Materials and Methods. Immunonegative cell bodies from the mLNTB and hLNTB were grouped together and compared to immunopositive cell bodies from the mLNTB and pvLNTB. The pvLNTB did not contain immunonegative cells. The number of puncta contacting immunonegative cells was significantly greater than the number contacting immunopositive cells of either the mLNTB or pvLNTB (ANOVA using BonFerroni adjustment for multiple inference; $P < .001$). Values are reported as mean ± standard deviation.

glycine, such as GABA, taurine or alanine, which can insert into the poly GLY-glutaraldehyde complex that may be necessary for antibody recognition (Ottersen et al., 1986), (2) the kinetics of manufacture and transport of neurotransmitter pools of glycine from the cell body, and (3) the size of metabolic pools of glycine which in some cells may reach the detection threshold by immunocytochemistry.

Regardless of the basis for variations in glycine immunolabeling intensity, correlation of this parameter with cell populations has been documented. In thin sections of the retina processed similarly to material used in the present study, variations of GLY-LI intensity was found among the population of amacrine cells (Pourcho and Goebel, 1990). The amacrine cell type exhibiting the darkest GLY-LI is referred to as A8, a cone dominated cell which contacts off-center ganglion cells. Medium intensity GLY-LI is associated with the A4 amacrine cell type, which contacts cone bipolar and off-center ganglion cells. Light GLY-LI is associated with the A3 and A7 amacrine cell populations. These populations of amacrine cells differ most notably in their postsynaptic targets, and therefore constitute different circuit elements that most likely subsume different functions in retinal information processing. Variations in the intensity of GLY-LI might, then, indicate morphological and functional classes of neurons in cell groups other than the retina.

Functional implications of dark GLY-LI

The intensity of immunolabeling in the pvLNTB is on a par with principal cells of the MNTB, whose demonstrated inputs to the lateral superior olive have been shown to utilize glycinergic neurotransmission (Caspary, 1990). Similarities in Nissl staining characteristics between pvLNTB cells and MNTB principal cells have been described (Taber, 1961; Warr, 1972; Adams, 1983; Spirou and Berrebi, 1996). Moreover, both cell types are contacted by large afferent terminals that are GLY- and GABA-immunonegative: calyces of Held in the case of MNTB principal cells (Held, 1893) and large endings resembling the modified endbulbs of cochlear nerve fibers (Ryugo and Rouiller, 1988) in the case of pale oval cells of the pvLNTB (Spirou and Berrebi, 1996). The calyces of Held are synaptic specializations of cochlear nucleus globular bushy cells, and the large endings in the pvLNTB originate in part (Smith et al., 1991; Berrebi and Spirou, 1994), and perhaps entirely, from the same cell type. The MNTB principal cells play roles in sound localization based on interaural intensity and timing cues through their inhibitory projections to the lateral superior olive and medial superior olive, and generate output patterns that are able to follow the temporal characteristics of the stimulus (Guinan et al., 1972a,b; Wu and Kelly, 1991; Banks and Smith, 1992). Cells of the

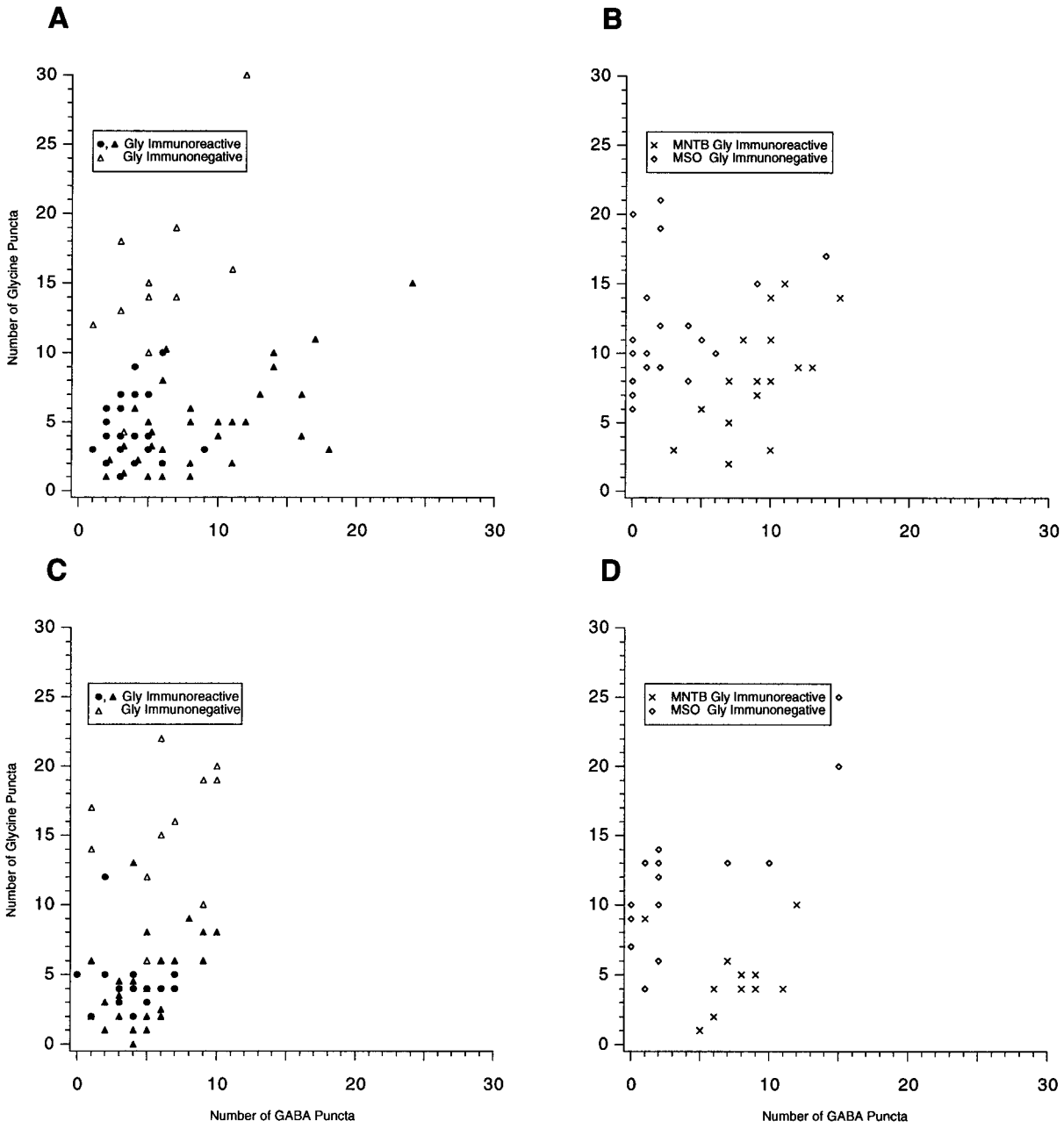

Fig. 10. Joint distribution of numbers of puncta displaying GLY-LI and GABA-LI apposed to GLY-LI and GLY-immunonegative cell bodies from two pairs of sections from each of two cats (animal #1: **A**,**B**; animal #2: **C**,**D**). In the LNTB (A,C), more GLY-LI than GABA-LI puncta contact GLY-immunonegative cell bodies (open triangles, cells found in mLNTB and hLNTB). Fewer GLY-LI than GABA-LI puncta contact GLY-LI cell bodies (filled circles, cells found in pvLNTB; filled triangles, cells found in mLNTB). (B,D) In the MSO, GLY-immunonegative cells are contacted by more GLY-LI than GABA-LI puncta. In the MNTB, darkly GLY-LI cells are contacted by roughly equal numbers of GLY-LI and GABA-LI puncta. Abbreviations as in Figures 1 and 2.

pvLNTB may exhibit membrane electrical characteristics consistent with generating these output patterns (Spirou et al., 1995a); however, it is unclear whether these neurons project into the lateral superior olive and medial superior olive. Ipsilateral inhibitory inputs to the medial superior olive (Goldberg and Brown, 1969; Yin and Chan, 1990) and lateral superior olive (Brownell et al., 1979) have been proposed and may arise from the LNTB (Cant, 1991; Smith, 1995). Therefore, the pvLNTB cells may form a population of neurons which are activated by the same auditory stimuli and generate similar output patterns as MNTB principal cells.

Glycine utilized as a neurotransmitter may play a specialized role in the function of cells of the MNTB and pvLNTB. If true, then the high levels of glycine reported in the somata of these cells by immunocytochemistry might be expected to reflect a greater concentration of glycine in the nerve terminals and perhaps the amount of synapti-

cally released glycine than is found in other neurons utilizing this neurotransmitter. Certain aspects of glycinergic neurotransmission may be important to the timing pathways of the auditory system. Desensitization occurs more rapidly when glycine receptors are exposed to higher glycine concentrations, and at least two glycine molecules may be necessary to activate the associated chloride channel (Bormann, 1990). Also, the binding affinity of glycine to the receptor may increase as the density of receptors in the postsynaptic membrane increases (Taleb and Betz, 1994). Although indications are that glycine and GABA receptors are linked to the same ion channel structure (Grenningloh et al., 1987; Schofield et al., 1987), the maximum conductance state of the glycine activated channel (45 pS) is greater than that measured for the GABA activated channel (30 pS) (Hamill et al., 1983; Bormann, 1990). All of the aforementioned factors may mitigate in favor of glycine, found in high levels in the presynaptic neuron, as the inhibitory transmitter of choice in the auditory system timing pathways, especially when the inhibitory input must compete with substantial numbers of synchronous excitatory inputs. Although the concentration of glycine in the synaptic cleft is probably regulated by several mechanisms, including rapid reuptake (Jursky and Nelson, 1995; Zafra et al., 1995), physiological investigations of glycinergic neurotransmission in the superior olive may be a fruitful area of study.

Other possible roles of glycinergic neurons in the auditory system

Glycinergic neurotransmission may also play a role in modulation of NMDA glutamate receptors, although it is unclear whether activation of the glycine binding site of this receptor occurs via such mechanisms as co-release of glutamate and glycine from the same nerve terminal (Ottersen et al., 1988), diffusion of glycine from an adjacent synaptic cleft, regulation of endogenous glycine levels by glycine transporters or the release of other agonists such as serine from glial cells (Schell et al., 1995). NMDA receptor proteins have been localized to the cochlear nucleus and superior olive using immunocytochemical techniques (Petralia et al., 1994a,b). The auditory brainstem, with its large numbers of cells showing GLY-LI and the prevalence of neurons thought to use glutamate as their neurotransmitter (Ottersen et al., 1995), may be one location at which neural modulation of the glycine binding site of NMDA receptors can occur.

Colocalization of GLY-LI and GABA-LI in the LNTB

Cell bodies exhibiting GABA-LI constitute a subset of cell bodies exhibiting GLY-LI, representing under half of mLNTB cells and about 30% of LNTB cells overall (based on cell counts from Spirou and Berrebi, 1996). The range of GABA immunolabeling intensity is smaller than that seen for GLY-LI, because there are virtually no darkly immunolabeled cells. In fact, many of the cells exhibited light GABA-LI, so the percentage of cells that could be identified confidently as GABAergic may be lower. The colocalization of these amino acids is a theme of increasing prevalence, and has been described in other structures of the auditory brainstem (for review, see Ottersen et al., 1995). Despite the fewer numbers of cell bodies exhibiting GABA-LI than GLY-LI, the prevalence of GABA-LI puncta indicates that GABA neurotransmission may play an important role in the function of the LNTB.

LNTB neurons inhibit their targets

Since about 85% of neurons of the LNTB exhibit GLY-LI, consideration of this nucleus as being inhibitory to its targets (Wenthold et al., 1987; Helfert et al., 1989) may be largely correct. We find smaller numbers of neurons showing GABA-LI than GLY-LI within the LNTB, consistent with other reports (Helfert et al., 1989). We also show that neurons that are GLY-immunonegative are also GABA-immunonegative (about 15% of all LNTB neurons) and may form excitatory projections to their targets. The presence of relatively few cells that show GABA-LI but which are GLY-immunonegative may be a common feature of auditory brainstem structures (Osen et al., 1990; Kolston et al., 1992; Moore et al., 1996).

Although ascending innervation of the LNTB originates strictly in the ventral cochlear nucleus, the descending projection from the LNTB terminates in all subdivisions of the cochlear nucleus (Spangler et al., 1987; Spirou and Berrebi, 1995; Spirou et al., 1995b) and may have pervasive effects on its function. Since an estimated 8,000 LNTB neurons in cats project to the cochlear nucleus (Spangler et al., 1987), and the entire cat LNTB contains roughly 9,000 neurons (Spirou and Berrebi, 1996), one would expect the subnucleus containing the largest number of neurons, the mLNTB (roughly 7,100 neurons), to contain most of the neurons projecting from the LNTB to the cochlear nucleus. The pale oval cells of the pvLNTB do form part of the projection from the LNTB to the cochlear nucleus in guinea pigs (Schofield, 1995), but may not in cats (Adams, 1983). The presence of many GLY-LI neurons in the LNTB is consistent with considerable retrograde labeling following injections of ^{3}H-glycine into the cochlear nucleus (Potashner et al., 1993). As many as 3,100 mLNTB neurons colocalize GLY-LI and GABA-LI (44% of 7,100 neurons). These neurons may contribute some of the many synaptic terminals in the cochlear nucleus that colocalize GABA-LI and GLY-LI (Kolston et al., 1992; Altschuler et al., 1993). In addition, cells of the LNTB have been shown to project into the medial superior olive in cats (Cant, 1991), although the locations of neurons retrogradely labeled from the cochlear nucleus and medial superior olive can not be evaluated with respect to our recently proposed parcellation scheme.

Neural circuitry

A striking feature of the GLY-LI patterns in the superior olive is the presence of immunoreactive puncta on nearly every neuron in the structures we examined, including the LNTB, MNTB, lateral superior olive, and medial superior olive. The tendency for cell bodies showing GLY-LI to be contacted by relatively few GLY-LI puncta has been quantified for cells of the lateral superior olive (Saint Marie et al., 1989). Within the lateral superior olive this demonstration is especially striking, since the densest accumulation of inhibitory inputs, as assessed using ultrastructural criteria, are found on the cell body (Cant, 1984). The projections of amacrine cells of the retina may be similarly organized (Hendrickson et al., 1988). The relative numbers of GLY-LI and GABA-LI puncta on cell bodies also correlates with the GLY-LI characteristics of the cell somata (Fig. 10), and is consistent across several nuclei of the superior olive.

Most likely the GLY-LI puncta within the LNTB originate intrinsically or from other periolivary nuclei, since the regions of the cochlear nucleus and inferior colliculus known to provide inputs to the LNTB are largely GLY immunonegative (Osen et al., 1990; Kolston et al., 1992; Winer et al., 1995). GABA-LI puncta may originate intrinsically, but also from other periolivary nuclei, since rostral structures, such as the inferior colliculus, provide only a sparse descending innervation that displays morphological characteristics consistent with an excitatory projection (Vetter et al., 1993).

In summary, most neurons of the LNTB exhibit GLY-LI. The spatial distribution of neurons that fall into different GLY-LI intensity categories correlates with subdivisions of the LNTB determined using independent techniques. In the MNTB, which is composed primarily of GLY-LI neurons, GABAergic inputs are thought to inhibit glycinergic cells (Adams and Mugnaini, 1990). Assuming that immunoreactivity reflects neurotransmitter phenotypes, within the LNTB glycinergic neurons (including cells that colocalize GABA) may determine one activity state in which their excitation suppresses non-glycinergic neurons; GABAergic inputs may determine a second activity state by suppressing glycinergic neurons and disinhibiting non-glycinergic (possibly excitatory) neurons.

ACKNOWLEDGMENTS

We thank Drs. Enrique Saldaña and Aric Agmon for critical reading of an early version of the manuscript and Dr. Gerald Hobbs for advice about statistical analyses. Stephanie Kessinger, Nancy Irby, Diane Berry, and Kevin Rowland provided technical assistance. Dr. David Pow kindly provided GABA antiserum and Drs. Jon Storm-Mathisen and Ole Ottersen kindly provided glycine antiserum.

LITERATURE CITED

Adams, J.C. (1983) Cytology of periolivary cells and the organization of their projections in the cat. J. Comp. Neurol. *215*:275–289.

Adams, J.C., and E. Mugnaini (1990) Immunocytochemical evidence for inhibitory and disinhibitory circuits in the superior olive. Hearing Res. *49*:281–298.

Altschuler, R.A., J.M. Juiz, S.E. Shore, S.C. Bledsoe, R.H. Helfert, and R.J. Wenthold (1993) Inhibitory amino acid synapses and pathways in the ventral cochlear nucleus. In M. A. Merchán, J. M. Juiz, D. A. Godfrey, and E. Mugnaini (eds): The Mammalian Cochlear Nuclei: Organization and Function. New York: Plenum Press, pp. 211–224.

Aoki, E., R. Semba, H. Keino, K. Kato, and S. Kashiwamata (1988) Glycine-like immunoreactivity in the rat auditory pathway. Brain Res. *442*:63–71.

Banks, M.I., and P.H. Smith (1992) Intracellular recordings from neurobiotin-labeled cells in brain slices of the rat medial nucleus of the trapezoid body. J. Neurosci. *12*:2819–2837.

Berrebi A.S., and G.A. Spirou (1994) PEP-19 immunolabeling of VCN bushy cells and their terminals in the superior olivary complex of the cat. Soc. Neuroscience Abstr. *20:*975.

Bormann, J. (1990) Patch-clamp studies of glycine-gated chloride channels. In O.P. Ottersen and J. Storm-Mathisen (eds): Glycine Neurotransmission. New York: John Wiley and Sons, pp. 111–138.

Brownell, W.E., P.B. Manis, and L.A. Ritz (1979) Ipsilateral inhibitory responses in the cat lateral superior olive. Brain Res. *177*:189–193.

Campistron, G., R.M. Buijs, and M. Geffard (1986) Glycine neurons in the brain and spinal cord. Antibody production and immunocytochemical localization. Brain Res. *376*:400–405.

Cant, N.B. (1984) The fine structure of the lateral superior olivary nucleus of the cat. J. Comp. Neurol. *227*:63–77.

Cant, N.B. (1991) Projections to the lateral and medial superior olivary nuclei from the spherical and globular bushy cells of the anteroventral cochlear nucleus. In R.A. Altschuler, R.P. Bobbin, B.M. Clopton and D.W. Hoffman (eds): Neurobiology of Hearing: The Central Auditory System. New York: Raven Press, pp. 99–120.

Cant, N.B., and R.L. Hyson (1992) Projections from the lateral nucleus of the trapezoid body to the medial superior olivary nucleus in the gerbil. Hearing Res. *58*:26–34.

Caspary, D.M. (1990) Electrophysiological studies of glycinergic mechanisms in auditory brainstem structures. In O.P. Ottersen and J. Storm-Mathisen (eds): Glycine Neurotransmission. New York: John Wiley and Sons, pp. 453–483.

Goldberg, J.M., and P.B. Brown (1969) Response of binaural neurons of dog superior olivary complex to dichotic tonal stimuli: Some physiological mechanisms of sound localization. J. Neurophysiol. *32*:613–636.

Grenningloh, G., A. Rienitz, B. Schmiott, C. Methfessel, M. Zensen, K. Meyreuther, E.D. Gundelfinger, and H. Betz (1987) The strychnine-binding subunit of the glycine receptor shows homology with nicotinic acetylcholine receptors. Nature *328*:215–220.

Guinan, J.J., S.S. Guinan, and B.E. Norris (1972a) Single auditory units in the superior olivary complex I. Responses to sounds and classifications based on physiological properties. Intern. J. Neuroscience *4*:101–120.

Guinan, J.J., B.E. Norris, and S.S. Guinan (1972b) Single auditory units in the superior olivary complex II: Locations of unit categories and tonotopic organization. Intern. J. Neuroscience *4*:147–166.

Hamill, O.P., J. Bormann, and B. Sakmann (1983) Activation of multiple-conductance state chloride channels in spinal neurones by glycine and GABA. Nature *305*:805–808.

Held, H. (1893) Die centrale Gehorleitung. Archiv fur Anatomie und Physiologie.

Helfert, R.H., J.M. Bonneau, R.J. Wenthold, and R.A. Altschuler (1989) GABA and glycine immunoreactivity in the guinea pig superior olivary complex. Brain Res. *501*:269–286.

Hendrickson, A.E., M.A. Koontz, R.G. Pourcho, P.V. Sarthy, and D.J. Goebel (1988) Localization of glycine-containing neurons in the *Macaca* monkey retina. J. Comp. Neurol. *273*:473–487.

Jursky, F., and N. Nelson (1995) Localization of glycine neurotransmitter transporter (GLYT2) reveals correlation with the distribution of glycine receptor. J. Neurochem. *64*:1026–1033.

Kallionatis, M., and E.L. Fletcher (1993) Immunocytochemical localization of the amino acid neurotransmitters in the chicken retina. J. Comp. Neurol. *336*:174–193.

Kolston, J., K.K. Osen, C.M. Hackney, O.P. Ottersen, and J. Storm-Mathisen (1992) An atlas of glycine- and GABA-like immunoreactivity and colocalization in the cochlear nuclear complex of the guinea pig. Anat. Embryol. *186*:443–465.

Lane, B.P., and D.L. Europa (1965) Differential staining of ultrathin sections of epon-embedded tissues for light microscopy. J. Histochem. Cytochem. *13*:579–582.

Luppi, P.-H., P.J. Charlety, P. Fort, H. Akaoka, G. Chouvet, and M. Jouvet (1991) Anatomical and electrophysiological evidence for a glycinergic inhibitory innervation of the rat locus coeruleus. Neurosci. Lett. *128*:33–36.

Moore, J.K., K.K. Osen, J. Storm-Mathisen, and O.P. Ottersen (1996) γ-Aminobutyric acid and glycine in the baboon cochlear nuclei: An immunocytochemical colocalization study with reference to interspecies differences in inhibitory systems. J. Comp. Neurol. *369*:497–519.

Osen, K.K., O.P. Ottersen, and J. Storm-Mathisen (1990) Colocalization of glycine-like and GABA-like immunoreactivities: A semiquantitative study of individual neurons in the dorsal cochlear nucleus of cat. In O.P. Ottersen and J. Storm-Mathisen (eds): Glycine Neurotransmission. New York: John Wiley and Sons, pp. 417–452.

Ottersen, O.P., O.P. Hjelle, K.K. Osen, and J.H. Laake (1995) Amino acid transmitters. In G. Paxinos (ed): The Rat Nervous System. New York: Academic Press, pp. 1017–1037.

Ottersen, O.P., and J. Storm-Mathisen (1984) Glutamate- and GABA-containing neurons in the mouse and rat brain, as demonstrated with a new immunocytochemical technique. J. Comp. Neurol. *229*:374–392.

Ottersen, O.P., J. Storm-Mathisen, S. Madsen, S. Skumlien, and J. Stromhaug (1986) Evaluation of the immunocytochemical method for amino acids. Med. Biol. *64*:147–158.

Ottersen, O.P., J. Storm-Mathisen, and P. Somogyi (1988) Colocalization of glycine-like and GABA-like immunoreactivities in Golgi cell terminals in the rat cerebellum: A post-embedding light and electron microscopic study. Brain Res. *450*:342–353.

Peters, A., S.L. Palay, and H. deF. Webster (1991) The Fine Structure of the Nervous System. New York: Oxford University Press.

Petralia, R.S., N. Yokotani, and R.J. Wenthold (1994a) Light and electron microscope distribution of the NMDA receptor subunit NMDAR1 in the rat nervous system using a selective anti-peptide antibody. J. Neurosci. *14*:667–696.

Petralia, R.S., Y.-X. Wang, and R.J. Wenthold (1994b) The NMDA receptor subunits NR2A and NR2B show histological and ultrastructural localization patterns similar to those of NR1. J. Neurosci. *14*:6102–6120.

Peyret, E., G. Campistron, M. Geffard, and J.M. Aran (1987) Glycine immunoreactivity in the brainstem auditory and vestibular nuclei of the guinea pig. Acta Otolaryngol. *104*:71–76.

Potashner, S.J., C.G. Benson, E.-M. Ostapoff, N. Lindberg, and D.K. Morest (1993) Glycine and GABA: Transmitter candidates of projections descending to the cochlear nucleus. In M.A. Merchán, J.M. Juiz, D.A. Godfrey and E. Mugnaini (eds): The Mammalian Cochlear Nuclei: Organization and Function. New York: Plenum Press, pp. 195–210.

Pourcho, R.G., and D.J. Goebel (1990) Autoradiographic and immunocytochemical studies of glycine-containing neurons in the retina. In O. P. Ottersen and J. Storm-Mathisen (eds): Glycine Neurotransmission. New York: John Wiley and Sons, pp. 355–390.

Pow, D.V., and S.R. Robinson (1994) Glutamate in some retinal neurons is derived solely from glia. Neuroscience *60*:355–366.

Ryugo, D.K., and E.M. Rouiller (1988) The central projections of intracellularly labeled auditory nerve fibers in cats: Morphometric correlations with physiological properties. J. Comp. Neurol. *271*:130–142.

Saint Marie, R.L., E.M. Ostapoff, D.K. Morest, and R.J. Wenthold (1989) Glycine-Immunoreactive projection of the cat lateral superior olive: Possible role in midbrain ear dominance. J. Comp. Neurol. *279*:382–396.

Schell, M.J., M.E. Molliver, and S.H. Snyder (1995) D-serine, an endogenous synaptic modulator: localization to astrocytes and glutamate-stimulated release. PNAS *92*:3948–3952.

Schofield, B.R. (1995) Bilateral projections to the cochlear nuclei from individual cells in the superior olivary complex. Neuroscience Abstr. *21*:673.

Schofield, P.R., M.G. Darlison, N. Fujita, D.R. Burt, F.A. Stevenson, H. Rodriguez, L.M. Rhee, J. Ramachandran, V. Reale, T.A. Glencorse, P.H. Seeburg, and E.A. Barnard (1987) Sequence and functional expression of the GABA-A receptor shows a ligand-gated super-family. Nature *328*:221–227.

Seguela, P., M. Geffard, R.M. Buijs, and M. Le Moal (1984) Antibodies against γ-aminobutyric acid: Specificity studies and immunocytochemical results. PNAS *81*: 3888–3892.

Smith, P.H. (1995) Structural and functional differences distinguish principal from nonprincipal cells in the guinea pig medial superior olive slice. J. Neurophysiol. *73*:1653–1667.

Smith, P.H., P.X. Joris, L.H. Carney, and T.C.T. Yin (1991) Projections of physiologically characterized globular bushy cell axons from the cochlear nucleus of the cat. J. Comp. Neurol. *304*:387–407.

Somogyi, P., A.J. Hodgson, I.W. Chubb, B. Penke, and A. Erdei (1985) Antisera to γ-aminobutryic acid. II. Immunocytochemical application to the central nervous system. J. Histochem. Cytochem. *33*:240–248.

Spangler, K.M., N.B. Cant, C.K. Henkel, G.R. Farley, and W.B. Warr (1987) Descending projections from the superior olivary complex to the cochlear nucleus of the cat. J. Comp. Neurol. *259*:452–465.

Spangler, K.M., and W.B. Warr (1991) The descending auditory system. In R.A. Altschuler, R.P. Bobbin, B.M. Clopton and D.W. Hoffman (eds): Neurobiology of Hearing: The Central Auditory System. New York: Raven Press, pp. 27–46.

Spirou, G.A., and A.S. Berrebi (1995) Anatomical basis for fast feedback from the lateral nucleus of the trapezoid body to the cochlear nucleus. In G. Manley, G. Klump, C. Köppl, H. Fastl, and H. Oeckinghaus (eds): Advances in Hearing Research. New Jersey: World Scientific, pp. 275–287.

Spirou, G.A., and A.S. Berrebi (1996) Organization of ventrolateral periolivary cells of the cat superior olive revealed by PEP-19 immunocytochemistry and Nissl stain. J. Comp. Neurol. *368*:100–120.

Spirou, G.A., P.H. Smith, and P.B. Manis (1995a) Intracellular recording and labeling of neurons in the lateral nucleus of the trapezoid body. Neurosci. Abstr. *21*:400.

Spirou, G.A., M.P. Walker, and A.S. Berrebi (1995b) Connectivity of the lateral nucleus of the trapezoid body in cats. ARO Abstracts *17*:87.

Storm-Mathisen, J., and O.P. Ottersen (1990) Antibodies and fixatives for the immunocytochemical localization of glycine. In O. P. Ottersen and J. Storm-Mathisen (eds): Glycine Neurotransmission. New York: John Wiley and Sons, pp. 281–302.

Taber, E. (1961) The cytoarchitecture of the brain stem of the cat. I. Brain stem nuclei of cat. J. Comp. Neurol. *116*:27–70.

Taleb, O., and H. Betz (1994) Expression of the human glycine receptor alpha1 subunit in Xenopus oocytes: Apparent affinities of agonists increase at high receptor density. EMBO J. *13*:1318–1324.

Vater, M. (1995) Ultrastructural and immunocytochemical observations on the superior olivary complex of the mustached bat. J. Comp. Neurol. *358*:155–180.

Vetter, D.E., E. Saldaña, and E. Mugnaini (1993) Input from the inferior colliculus to medial olivocochlear neurons in the rat: A double label study with PHA-L and cholera toxin. Hearing Res. *70*:173–186.

Warr, W.B. (1972) Fiber degeneration following lesions in the multipolar and globular cell areas in the ventral cochlear nucleus of the cat. Brain Res. *40*:247–270.

Wenthold, R.J., D. Huie, R.A. Altschuler, and K.A. Reeks (1987) Glycine immunoreactivity localized in the cochlear nucleus and superior olivary complex. Neuroscience. *22*:897–912.

Winer, J.A., D.T. Larue, and G.D. Pollak (1995) GABA and Glycine in the central auditory system of the mustache bat: Structural substrates for inhibitory neuronal organization. J. Comp. Neurol. *355*:317–353.

Wu, S.H., and J.B. Kelly (1991) Physiological properties of neurons in the mouse superior olive: Membrane characteristics and postsynaptic responses studied in vitro. J. Neurophysiol. *65*:230–246.

Yin, T.C.T., and J.C.K. Chan (1990) Interaural time sensitivity in medial superior olive of cat. J. Neurophysiol. *64*:465–488.

Zafra, F., C. Aragon, L. Olivares, N.C. Danbolt, C. Gimenez, and J. Storm-Mathisen (1995) Glycine transporters are differentially expressed among CNS cells. J. Neurosci. *15*:3952–3969.